Roll-to-roll manufacturing of disposable surface-enhanced Raman scattering (SERS) sensors on paper based substrates

Jarkko J. Saarinen, Dimitar Valtakari, Simon Sandén, Janne Haapanen, Turkka Salminen, Jyrki M Mäkelä, and Jun Uozumi

KEYWORDS: Surface-enhanced Raman scattering (SERS), Silver nanoparticle, Paper, Flexography, Inkjet, Liquid flame spray (LFS)

ABSTRACT: We present two cost-effective routes for roll-to-roll (R2R) manufacturing of silver nanoparticle based surface-enhanced Raman scattering (SERS) active substrates on paper utilizing either inkjet printing or liquid flame spray (LFS) nanoparticle deposition. Paper is cost-effective, renewable, recyclable, and biodegradable that can easily be disposed after the SERS analysis. Paper based substrates can have a strong luminescence that can overshadow the rather weak SERS signal. Two solutions are presented here that solve the luminescence issue of the base paper substrate. A full silver coverage by inkjet printing or alternatively a simple flexography carbon coating can suppress the background luminescence allowing a reliable SERS characterization. The detection limit of the sample analyte crystal violet was 100 nM corresponding to 100 fmol in a 1 µl sample volume. These approaches can provide a cost-effective route towards disposable, point-of-care SERS active substrates.

ADDRESSES OF THE AUTHORS: Jarkko J. Saarinen (jarkko.j.saarinen@abo.fi), **Dimitar Valtakari** (dimitar.valtakari@abo.fi): Center for Functional Materials at Biological Interfaces (FunMat), Laboratory of Paper Coating and Converting, Faculty of Science and Engineering, Abo Akademi University, Porthansgatan 3, FI-20500 Turku, Finland. **Simon Sandén** (simon.sanden@abo.fi): Center for Functional Materials at Biological Interfaces (FunMat), Physics, Faculty of Science and Engineering, Abo Akademi University, Porthansgatan 3, FI-20500 Turku, Finland. **Janne Haapanen** (janne.haapanen@tut.fi), **Jyrki M. Mäkelä** (jyrki.makela@tut.fi): Aerosol Physics Laboratory, Department of Physics, Tampere University of Technology, P. O. Box 692, FI-33101 Tampere, Finland. **Turkka Salminen** (turkka.salminen@tut.fi), Optoelectronics Research Centre, Tampere University of Technology, P. O. Box 692, FI-33101 Tampere, Finland **Jun Uozumi** (uozumi@eli.hokkai-s-u.ac.jp): Faculty of Engineering, Hokkai-Gakuen University, South-26, West-11, Chuo-ku, Sapporo 064-0926, Japan.
Corresponding author: Jarkko J Saarinen

Introduction

Cellulose is the most abundant biopolymer on Earth. The benefits of natural fibre based substrates such as paper and paperboard include recyclability, renewability, biodegradability, and such substrates can be produced at a large scale cost-effectively. In recent years research and development has shifted towards value-added products such as printed electronics and printed functionality on natural fibre based substrates for low-cost and disposable electronics (Tobjörk, Österbacka 2011; Martins et al. 2011; Martins et al. 2013). For example, recyclable solar cells have been demonstrated on a cellulose nanocrystal substrate with 2.7% solar power conversion efficiency (Zhou et al. 2014) or on cast coated papers with 3.4% solar power conversion efficiency (Aguas et al. 2015).

Recently paper has found an increasing number of applications in the point-of-care (POC) diagnostics. Porosity of paper is an advantage as the capillary pressure can be utilized for liquid actuation e.g. in microfluidic paper-based analytical devices (µPADs) (Martinez et al. 2010), for colorimetric detection of liver markers (Vella et al. 2012) or electrochemically active bacteria (Marques et al. 2015) using a micropatterned paper, or enzymatic reactions, immunoassays, and nucleic acid sequence identification (Costa et al. 2014). Blood typing has also been realized on paper by stabilizing antibodies onto paper (Khan et al. 2010; Guan et al. 2014). An additional benefit of paper is easy disposability by combustion after sample analysis leaving no hazardous biowaste.

POC analysis can also be based on detection of Raman scattering originating from inelastically scattered photons that are coupled to the vibrational modes of the molecules. Thus a Raman spectrum yields a spectral fingerprint of the studied substance allowing accurate identification of the samples (Lewis, Edwards 2001). Raman scattering takes place when there is a change in the polarizability of the molecule whereas conventional infrared spectroscopy is based on the change in the dipole moment. Therefore, aqueous solutions can easily be measured using Raman spectroscopy. Unfortunately, a significant drawback with Raman spectroscopy is the weak signal levels as only one photon in approximately 10 million experiences inelastic scattering.

Various approaches have been taken to enhance the Raman signal using plasmonic metallic nanostructures such as nanoparticles, tips, or roughened surfaces that enhance the local electric field intensity and thus, Raman scattering (Kneipp et al. 2006). Recently Raman spectroscopy has been incorporated with microfluidic devices for detection of food-borne pathogens (Mungroo et al. 2016) and for malaria diagnosis (Yuen, Liu 2013).

Traditionally surface-enhanced Raman scattering (SERS) is observed on metal nanoparticle coated glass substrates. In a typical Raman measurement the sample stains the SERS active substrate and can only be used once. To lower the cost of such SERS analysis silver nanoparticles were inkjet printed on purified cellulose substrate (Yu, White 2010) with sensitivity down to femtomolar level with a rhodamine test analyte. Silver nanoparticles have also been used on cardboard packages with metal surface for highly efficient SERS response

(Araujo et al. 2014). Alternatively gold nanoparticles have been utilized for SERS activation on qualitative filter paper (98% pure cellulose) to minimize the interference with paper coating (Ngo et al. 2013; Ngo et al. 2013b) for cost-effective bio-diagnostic applications. In recent years there has been a growing interest in paper-based SERS analysis (Polavarapu et al. 2014; Torul et al. 2015; Villa, Poppi 2016).

In this paper we utilize two different routes for generation of low-cost, large-area SERS active substrates. First, inkjet printing with commercial silver nanoparticle ink is studied on paperboard. We have previously shown (Saarinen et al. 2014) that inkjet is suitable for making SERS active substrates on a glass substrate. Secondly, a liquid flame spray (LFS) silver nanoparticle deposition (Mäkelä et al. 2011) is utilized that allows cost-effective deposition of various metal and metal oxide nanoparticles in atmospheric conditions in a roll-to-roll process flow. LFS contains a high temperature and a high velocity flame in which an organometallic precursor evaporates, nucleates, and forms solid nanoparticles. These nanoparticles can be deposited on various substrates, and LFS has been utilized e.g. for controlled wetting of paperboard with TiO_2 nanoparticles (Stepien et al 2011; Stepien et al 2012; Stepien et al. 2013; Valtakari et al. 2016).

A common problem with paper for SERS analysis is signal crowding due to high fluorescence and luminescence from the base paper components such as organic binders, inorganic fillers, and additives. These can overshadow the SERS signal. We present here two different routes to solve the luminescence issue: first, inkjet printing of silver nanoparticles with sufficiently small drop spacing distance results in a rather uniform silver layer on top of paper that also prevents luminescence generation. A more cost-efficient and biocompatible solution is also presented as we apply a simple graphite coating using flexography. A thin carbon coating is adequate to suppress the luminescence, and thus the SERS signal can be measured from substrates with significantly lower amount of deposited silver. Finally, it would also be possible to use a time-gated Raman measurement (Knorr et al. 2010; Kostamovaara et al. 2013) as Raman scattering has a lifetime in femtosecond range whereas luminescence is within the picosecond range. Hence by limiting the signal collection to less than picosecond the Raman signal can be collected. However, this sets additional requirements for the measurement system, and may limit applicability of the technology for POC applications.

Materials and Methods

Sample preparation

Fig 1 shows a schematic picture of the liquid flame spray process (a) and inkjet printer (b) used in preparation of the silver nanoparticle deposited SERS active substrates. Furthermore, a laboratory scale flexography test printer used for carbon coating is shown in *Fig 1* (c). All SERS active structures were fabricated on a commercially available double pigment coated paperboard (200 g/m^2, Stora Enso, SE) containing both calcium carbonate ($CaCO_3$) and kaolin clay mineral pigment particles in the coating recipe.

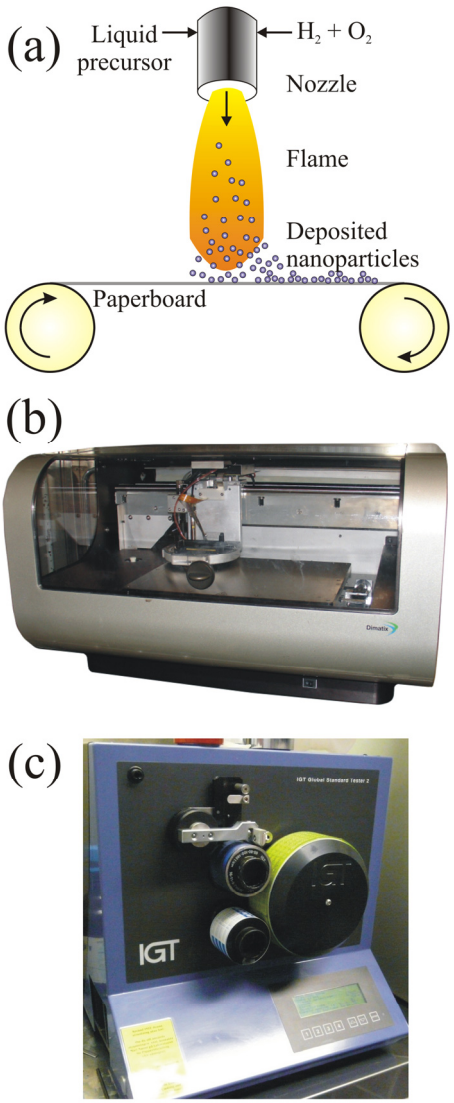

Fig 1 - A schematic picture of the (a) LFS silver nanoparticle deposition system, (b) the used inkjet printer with the silver nanoparticle ink, and (c) the used laboratory scale flexography printer for graphite carbon coating.

Liquid flame spray (LFS) Ag nanoparticle deposition

Here two different particle sizes were deposited using silver nitrate ($AgNO_3$, 99.9+%, Alfa Aesar) precursor in water solution that was fed into the flame with a silver concentration of 750 mg/ml in the precursor and gas flow ratios of 55 l/min (H_2) and 5 l/min (O_2) were used to synthesize silver nanoparticles with an average diameter of 90 nm with a fixed precursor feed rate of 4 ml/min. The silver precursor concentration was reduced to 500 mg/ml with the gas flow ratios of 40 l/min (H_2) and 20 l/min (O_2) with a fixed precursor feed rate of 2 ml/min were used for deposition of Ag nanoparticles with an average diameter of 50 nm.

Inkjet printing and thermal curing of the silver surface

Silver nanoparticles were inkjetted using a commercial ethanol based 20 wt.% silver nanoparticle ink having 20 to 50 nm particle size distribution (SunTronic Jettable Silver U5603, Sun Chemical Electronic Materials, Sun Chemical Ltd., UK). The inkjet printing was carried out with a piezoelectric Dimatix DMP-2800 (Fujifilm Dimatix Inc., US) on a drop-on-demand mode. A single nozzle with 10 pl drop volume with three different drop spacing values of 45, 60, and 85 μm were applied on paperboard substrate. The paperboard samples were cured for 30 min in an oven with a temperature of 120°C. We have previously shown with glass samples (Saarinen et al. 2014) that a higher curing temperature of 200°C resulted in a carbon layer on top of the Ag nanoparticles on glass slides that suppressed the SERS signal generation. Thus 120°C was utilized with paperboard samples.

Carbon coating by graphite ink

Carbon coatings were performed on a paperboard using a laboratory scale flexography IGT GST 2 printability tester (IGT Testings Systems, NL) as shown in *Fig 1(c)*. The anilox cylinder had a cell angle of 45° with 40 lines/cm and volume of 20 ml/m^2. The graphite ink was a resistor ink suitable for flexography and rotogravure (110-04, Creative Materials, US). The ink was coated at a print speed of 1.0 m/s with successive prints up to four times. The pressure between the anilox cylinder and the printing plate was set to 50 N whereas the pressure between the printing plate and the substrate was set to 100 N.

Photoluminescence and SEM measurements

Photoluminescence of the plastic film and paperboard with and without flexography carbon coating were measured using an Olympus BX60 fluorescence microscope (Olympus, JP) with a 490 nm laser excitation wavelength. The scanning electron microscopy (SEM) imaging was carried out using a Carl Zeiss Ultra-55 microscope (Carl Zeiss AG, DE) with a secondary electron (SE) detector for surface imaging, and an integrated energy and angle selective backscattered electron (ESB) detector for compositional information. Both for surface morphology and composition imaging an acceleration voltage and magnification of 1.00 kV and 10 kX were utilized, respectively. For the ESB imaging an energy window width of 482 eV was used.

Raman spectroscopy

Raman spectroscopy was carried out with a spectrometer (Andor Shamrock 303) and a cooled charge-coupled device (CCD) camera (Newton 940P). The Raman excitation was performed using a 532 nm wavelength Cobolt Samba laser. The sample was illuminated with a collimated laser beam in an approximately 30° angle with respect to the sample surface. The scattered light was collected with a microscope objective along the normal of the surface of the sample and Rayleigh scattered light was filtered out with a Semrock Razoredge filter. The laser spot size on the sample surface was approximately 700 μm.

We utilized crystal violet (CV, CAS [548-62-9], Sigma-Aldrich, USA) diluted in deionized distilled water (Millipore 18.2 MΩ, Merck Millipore, USA) as a test analyte for detection of SERS signal. CV concentrations of 1 μM, 100 nM, and 10 nM in water were used. A 5 μl micropipet (Hamilton, Reno, USA) was used to place a 1 μl droplet of the sample analyte onto the surface with an average droplet diameter on the sample surface of approximately 2–3 mm. SERS measurements were acquired after the droplet had dried on the surface. The SERS spectrum was measured from three different spots of the dried sample analyte and average signal from these three measurements are shown.

Results and Discussion

Inkjet printed Ag samples on paperboard

Fig 2 shows the average SERS signals measured on inkjet printed silver nanoparticle samples on paperboard surface as a function of the increased drop spacing (DS) from 45 μm to 85 μm with three different sample CV analyte concentrations of 1 μM, 100 nM, and 10 nM. The lower row image shows the corresponding optical microscope images taken using the microscope of the Dimatix DMP-2800 inkjet printer after the sample manufacturing. A significant increase in the total number of counts is observed as the drop spacing increases. This is expected as with higher drop spacing the background paperboard surface is more exposed to the electromagnetic excitation as shown in the lower row in *Fig 2* also displaying the used laser spot size.

We have shown in our previous study (Saarinen et al. 2014) that the printed silver droplet is fully covered by silver nanoparticles with diameters from 30 to 50 nm. It is possible to estimate the silver amount in the coatings with different spot sizes. The used ink contains 20 wt.% of silver mixed together with ethanol, ethylene glycol and glycerol. Using the typical densities of the substances the deposited silver amount of the surface is 1300, 730, and 360 mg/m^2 for DS 45, 60, and 85 μm, respectively.

The top layer of the used commercial pigment coated paperboard consists of mineral calcium carbonate and kaolin clay pigments verified by the X-ray photoelectron spectroscopy (Stepien et al. 2012) that are immersed in an organic binder, typically styrene butadiene or styrene acrylic latex. Kaolin clay exhibits a strong fluorescence and photoluminescence (Vyörykkä 2004; Vyörykkä et al. 2004). Hence, the characteristic Raman signal is lost in the strong luminescence background, and the photoluminescence becomes the main signal source with increased drop spacing. For the paperboard sample with a full silver coverage using a 45 μm drop spacing, we have a peak contrast (peak signal compared to background signal level) of 1.47 and 2.02 for the 10 nM CV peaks at 1586 cm^{-1} and 1618 cm^{-1}, respectively. The peak contrast to background signal level was determined from the baseline in the vicinity of the investigated peak using interpolation with the second derivatives. No other spectral processing or normalization was performed.

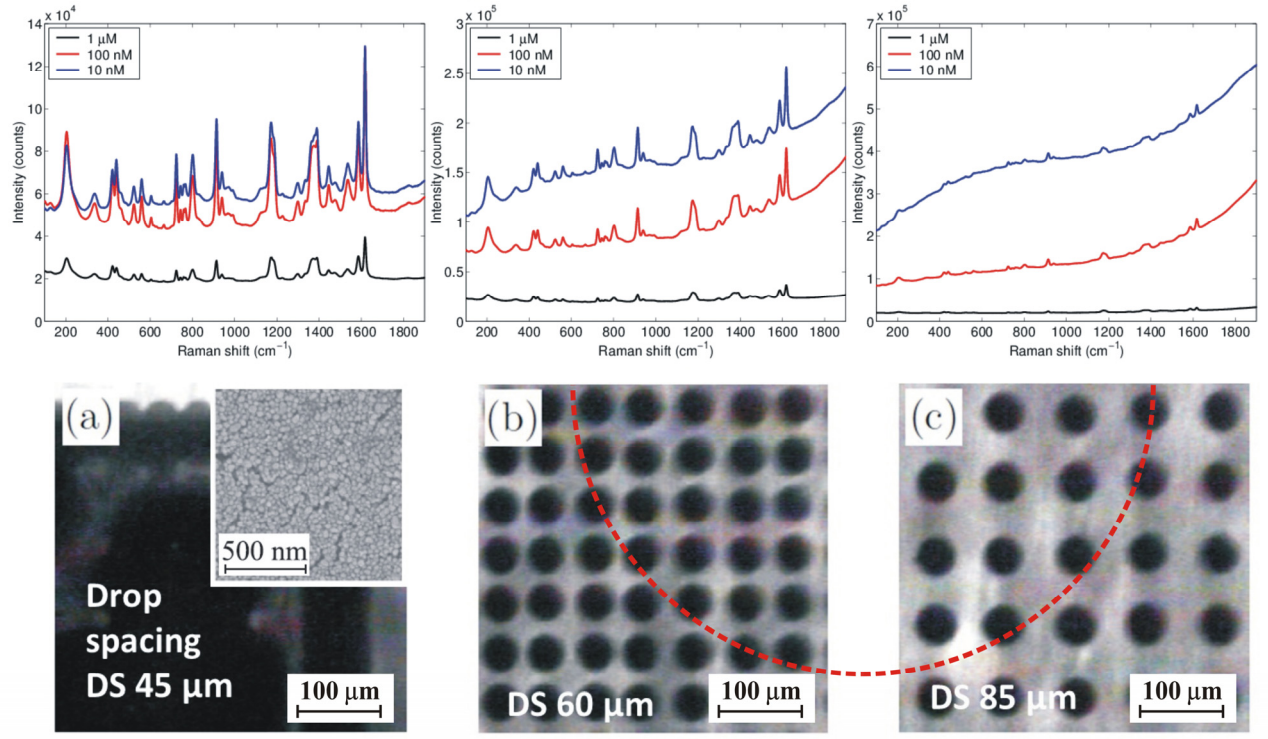

Fig 2 - SERS signal from inkjet printed Ag nanoparticles on paperboard with increasing drop spacing value from 45 µm (a) to 85 µm (c). The subfigure in (a) shows a high magnification image inside the printed drop with full coverage of nanoparticles. The dashed red circle in (b) and (c) displays the laser spot size on the sample surface used in the Raman measurements.

These findings are almost on a similar signal level compared to the inkjet printed glass samples with 45 µm drop spacing presented in our previous paper (Saarinen et al. 2014) that had a characteristic peak contrast of 1.57 at 1586 cm^{-1} and 2.33 at 1618 cm^{-1} for the 10 nM CV solution. Unfortunately, these detection levels drop drastically as silver drop spacing increases: with 85 µm drop spacing the characteristic peak contrasts are 1.20 at 1586 cm^{-1} and 1.31 at 1618 cm^{-1} even for 1 µM concentration. The different CV concentrations show an expected result with the highest CV concentration resulting in the highest SERS activity.

LFS deposited Ag nanoparticles on carbon coated paperboard

Fig 2 clearly shows that increasing the drop spacing value of the Ag inkjet printing resulted in a lost SERS signal below the background luminescence from the paperboard. Therefore, depositing individual silver nanoparticles using the LFS nanoparticle deposition as shown in our previous paper (Saarinen et al. 2014) on paperboard did not result in a measurable SERS spectrum. To overcome the luminescence issue a cost-effective graphite carbon coating was utilized.

Fig 3 shows the measured photoluminescence signal from the reference paperboard compared to flexography carbon coated paperboard and a plastic Mylar films excited at 490 nm laser light. Paperboard has a strong luminescence around 550 nm emission wavelengths, which can be completely suppressed by the successive flexography printed carbon coatings. These have comparable luminescence values to a plastic film that has conventionally been used for Raman active substrates.

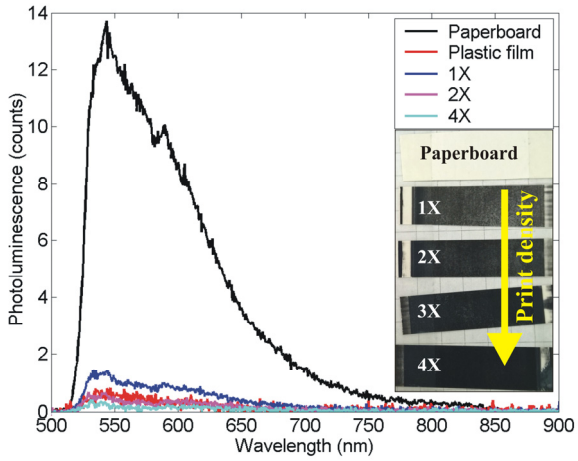

Fig 3 - Examples of the flexography printed carbon coatings on paperboard with increasing print density with the successive prints and the corresponding measured photoluminescence signal of the reference paperboard and the flexography printed carbon coatings with 1×, 2× and 4× carbon coating compared to the plastic film reference at excitation of 490 nm.

Even a single flexography print suppresses photoluminescence significantly but two successive flexography prints result in an almost perfect blocking layer for the photoluminescence. Optimizing the used flexography printing parameters (anilox and ink properties) it is possible to have adequate photoluminescence suppression even with a single print.

LFS is a versatile method for producing single (Tikkanen et al. 1997) or multi-component (Haapanen et al. 2015) nanoparticles. The formed nanoparticle size can

be controlled via the process parameters including the flow rates of the gases and precursor, precursor concentration, and deposition time and burner distance from the substrate. An additional benefit of the LFS process is that the generated nanoparticles can be collected on a moving web, which allows large areas to be coated via roll-to-roll process flow.

Fig 4 shows the SE and ESB images of the carbon coated paperboard (a) and the corresponding carbon coated paperboard functionalized using the LFS deposited Ag NPs with (b) 10×90nm+10×50nm, (c) 25×90nm+10×50nm and (d) 50×90nm+10×50nm sweeps.

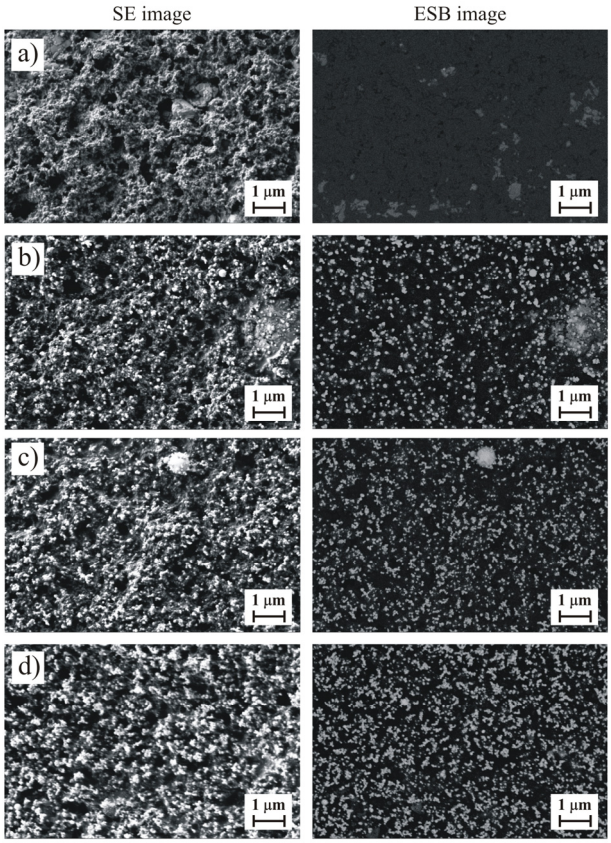

Fig 4 - Secondary electron (SE) and energy selective backscattered (ESB) images of carbon coated paperboard (a) and LFS deposited silver nanoparticle functionalized carbon coated paperboard with 10×90nm+10×50nm, 25×90nm+10×50nm, and 50×90nm+10×50nm silver nanoparticles in (b), (c), and (d), respectively.

The observed amount of Ag NPs correlates well with an increasing number of deposition sweeps for the 90 nm Ag NPs as clearly seen from the ESB images. The elementally heavier silver results in a stronger backscattering signal than carbon and thus, Ag NPs are seen as bright spots. Estimation from the used deposition parameters results in a surface coverage of 12%, 23%, and 43%. This corresponds to a silver amount of 60, 140 and 260 mg/m^2. Hence, the deposited amount of silver on the surface is significantly smaller compared to the inkjet printed samples. The nanoparticle coating is rather uniform with separate Ag NPs in *Fig 4(b)* and *(c)* excluding the larger cluster visible in *(c)* whereas the highest deposition amount with 50×90 nm Ag NP sweeps resulted in a formation of larger clusters as shown in *Fig 4(d)*. The highest deposition amount has also the highest exposure to the heat from the flame that may induce clustering.

The measured SERS signals for the LFS deposited Ag nanoparticle samples on a flexography printed carbon coated paperboard are presented in *Fig 5* with three different CV analyte concentrations of 1 µM, 100 nM, and 10 nM. Three different nanoparticle amounts are presented. The samples were deposited 50×, 25×, or 10× times by 90 nm Ag nanoparticles followed by 10× times deposition with 50 nm Ag nanoparticles. The number of LFS depositions correlates with the amount of deposited nanoparticles i.e. 50×90 nm LFS sample has twice the mass of 90 nm Ag NPs compared to 25×90 nm sample. All samples in *Fig 5* clearly show distinguishable CV peaks with the highest CV concentration of 1 µM. However, on a carbon coating the graphite G-band Raman excitation is visible especially with lower CV concentration around 1582 cm^{-1}, and the measured spectrum is a sum of CV and graphite peaks. Nevertheless, the two characteristic CV peaks are visible in all samples with 100 nM CV concentration. In a recent paper (Chen et al. 2014) the quality of Raman spectra with low signal-to-noise ratio were improved using four commonly used de-noising methods in Raman spectroscopy. A similar approach can be utilized with paper-based SERS spectra and we plan to return to this issue in future communication.

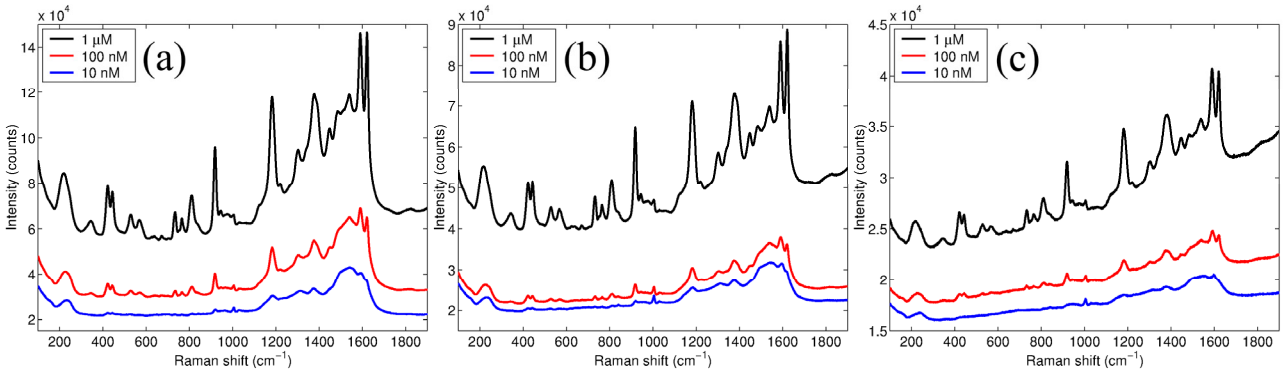

Fig 5 - Measured SERS intensities for (a) 50×90 nm + 10×50 nm, (b) 25×90 nm + 10×50 nm, and (c) 10×90 nm + 10×50 nm LFS deposited Ag nanoparticles on carbon coated paperboard.

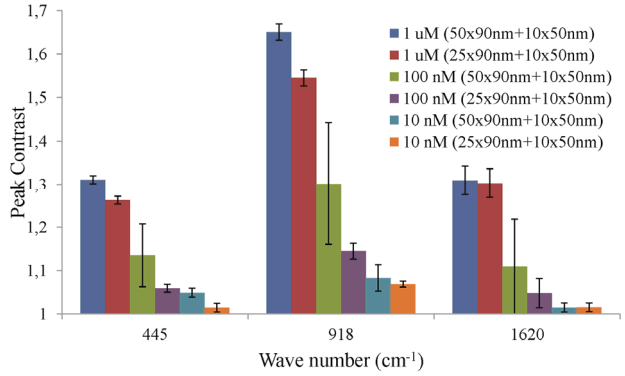

Fig 6 - The average peak to background contrast ratio with standard deviation for characteristic CV peaks of 445, 918 and 1618 cm-1 peaks for three different CV concentrations on carbon coated paper with two different LFS Ag nanoparticle amounts.

Finally, three different CV peaks at 445 cm^{-1}, 918 cm^{-1}, and 1618 cm^{-1} with three different CV concentrations were analyzed for 50×90nm+10×50nm and 25×90nm+10×50nm samples that are shown in *Fig 6.* The displayed peak contrast values are an average of three SERS measurements from different sample spots displayed with standard deviation. In both these samples the best peak constrast was observed for 918 cm^{-1} peak with a contrast value of approximately 1.6 for the 1 µM peak intensity compared to the background level. This analysis also verifies that with individual Ag nanoparticles on carbon coated paperboard a reliable detection range is in 1 µM range whereas with inkjet printed Ag samples 100 nM was still detectable. On the other hand, the LFS nanoparticle coatings have significantly less silver on the surface thus providing a large potential for cost savings.

Conclusions

We have investigated two different routes for manufacturing disposable SERS active substrates based on silver nanoparticles deposited on paperboard substrate. The issue of inherent luminescence from the paper substrates is solved using two different approaches. A full coverage of silver on the surface by inkjet printing with small enough drop spacing resulted in a detection limit of 100 nM of the sample crystal violet analyte. However, an increased drop spacing value in the inkjet printing resulted in a lower coverage of paperboard and thus a strong excitation of photoluminescence that overshadowed the SERS signal from the studied sample crystal violet analyte. On the other hand, a more cost-efficient flexography carbon graphite coating on paperboard was utilized to suppress the luminescence from the background paperboard substrate. On such carbon coated paperboard, the LFS deposited silver nanoparticles resulted in a detection limit of 1 µM of CV with a significantly reduced silver amount (and cost) compared to the inkjet printing with full surface coverage.

Our work shows avenues towards disposable, renewable, and sustainable cellulose based SERS active substrates. We believe that the developed SERS active substrates will find many applications in POC diagnostics in the future.

Acknowledgements

This work was supported by the Academy of Finland (grant nos 250 122, 256 263, and 283 054). Japan Society for the Promotion of Science (JSPS, BR151101) is acknowledged for a research visit to the Hokkai-Gakuen University, Sapporo, Japan. SS acknowledges support from the Academy of Finland project no. 37093 (POHSC).

References

Aguas, H,, Mateus, T., Vicente, A., Gaspar, D., Mendes M. J., Schmidt, W. A., Pereira, L., Fortunato, E., Martins, R. (2015): Thin film silicon photovoltaic cells on paper for flexible indoor applications, Adv. Funct. Mater. 25, 3592-3598.

Araujo, A., Caro, C., Mendes, M. J., Nunes, D., Fortunato, E., Franco, R., Aguas, H., Martins, R. (2014): Highly efficient nanoplasmonic SERS on cardboard packaging substrates, Nanotechnology 25, 415202.

Chen, S., Lin, X., Yuen, C., Padmanabhan, S., Beuerman, R. W., Liu, Q. (2014): Recovery of Raman spectra with low signal-to-noise ratio using Wiener estimation, Opt. Express 22, 12102-12114.

Costa, M. N., Veigas, B., Jacob, J. M., Santos, D. S., Gomes, J., Baptista, P. V., Martins, R., Inacio, J., Fortunato, E. (2014): A low cost, safe, disposable, rapid and self-sustainable paper-based platform for diagnostic testing: lab-on-paper, Nanotechnology 25, 094006.

Guan, L., Cao, R., Tian, J., McLiesh, H., Garnier, G., Shen, W. (2014): A preliminary study on the stabilization of blood typing antibodies sorbed into paper, Cellulose 21, 717-727.

Haapanen, J., Aromaa, M., Teisala, H., Tuominen, M., Stepien, M., Saarinen, J.J., Heikkilä, M., Toivakka, M., Kuusipalo, J., Mäkelä, J.M. (2015): Binary TiO_2/SiO_2 nanoparticle coating for controlling the wetting properties of paperboard. Mater. Chem. Phys. 149–150, 230–237.

Khan, M.S., Thouas, G., Shen, W., Whyte, G., Garnier, G. (2010): Paper diagnostic for instantaneous blood typing, Anal. Chem. 82, 4158--4164.

Kneipp, K., Moskovits, M., Kneipp, H. (2006): Surface-enhanced Raman scattering: Physics and applications, Springer, Heidelberg.

Knorr, F., Smith, Z.J., Wachsmann-Hogiu, S. (2010): Development of a time-gated system for Raman spectroscopy of biological samples, Opt. Express 18, 20049-20058.

Kostamovaara, J., Tenhunen, J., Kögler, M., Nissinen, L., Nissinen, J., Keränen, P. (2013): Fluorescence suppression in Raman spectroscopy using a time-gated CMOS SPAD, Opt. Express 21, 31632-31645.

Lewis, I.R., Edwards, H. (2001): Handbook of Raman spectroscopy: From the research laboratory to the process line, CRC Press, New York.

Marques, A. C., Santos, L., Costa, M. N., Dantas, J. M., Duarte, P., Goncalves, A., Martins, R., Salgueiro, C. A., Fortunato, E. (2015): Office paper platform for bioelectrochromic detection of electrochemically active bacteria using tungsten trioxide nanoprobes, Sci. Rep. 5, 9910.

Martinez, A.W., Phillips, S.T., Whitesides, G.M., Carrilho, E. (2010): Diagnostics for the developing world: Microfluidic paper-based analytical devices, Anal. Chem. 82, 3-10.

Martins, R., Ferreira, I., Fortunato, E., (2011): Electronics with and on paper, Phys. Status Solidi RRL 5, 332-335.

Martins, R. F. P., Ahnood, A., Correia, N., Pereira, L. M. N. P., Barros, R., Barquinha, P. M. C. B., Costa, R., Ferreira, I. M. M., Nathan, A., Fortunato, E. E. M. C., (2013): Recyclable, flexible, low-power oxide electronics, Adv. Funct. Mater. 23, 2153-2161.

Mungroo, N.A., Oliveira, G., Neethirajan, S. (2016): SERS based point-of-care detection of food-borne pathogens, Microchim. Acta.183, 697-707.

Mäkelä, J.M., Aromaa, M., Teisala, H., Tuominen, M., Stepien, M., Saarinen, J.J., Toivakka, M., Kuusipalo, J. (2011): Nanoparticle deposition from liquid flame spray onto moving roll-to-roll paperboard material, Aerosol Sci. Technol. 45, 817-827.

Ngo, Y.H., Li, D., Simon, G.P., Garnier, G. (2013): Effect of cationic polyacrylamides on the aggregation and SERS performance of gold nanoparticles-treated paper, J. Colloid Interf. Sci. 392, 237-246.

Ngo, Y.H., Then, W.L., Shen, W., Garnier, G. (2013b): Gold nanoparticles paper as a SERS bio-diagnostic platform, J. Colloid Interf. Sci. 409, 59-65.

Polavarapu, L., Porta, A.L., Novikov, S.M., Coronado-Puchau, M. and Liz-Marzán, L.M. (2014): Pen-on-paper approach toward the design of universal surface enhanced Raman scattering substrates, Small 10, 3065–3071.

Saarinen, J.J., Valtakari, D., Haapanen, J., Salminen, T., Mäkelä, J.M., Uozumi, J. (2014): Surface-enhanced Raman scattering active substrates by liquid flame spray deposited and inkjet printed silver nanoparticles, Opt. Rev. 21, 339-344.

Stepien, M., Saarinen, J.J., Teisala, H., Tuominen, M., Aromaa, M., Kuusipalo, J., Mäkelä, J.M., Toivakka, M. (2011): Adjustable wettability of paperboard by liquid flame spray nanoparticle deposition, Appl. Surf. Sci. 257, 1911-1917.

Stepien, M., Saarinen, J.J., Teisala, H., Tuominen, M., Aromaa, M., Kuusipalo, J., Mäkelä, J.M., Toivakka, M. (2012): Surface chemical analysis of photocatalytic wettability conversion of TiO_2 nanoparticle coating, Surf. Coat. Tech. 208, 73-79.

Stepien, M., Saarinen, J.J., Teisala, H., Tuominen, M., Aromaa, M., Haapanen, J., Kuusipalo, J., Mäkelä, J.M., Toivakka, M. (2013): ToF-SIMS analysis of UV-switchable TiO_2‑nanoparticle-coated paper surface, Langmuir 29, 3780-3790.

Tikkanen, J., Gross, K.A., Berndt, C.C., Pitkänen, V., Keskinen, J., Raghu, S., Rajala, M., Karthikeyan, J. (1997): Characteristics of the liquid flame spray process, Surf. Coat. Tech. 90, 210–216.

Tobjörk, D., Österbacka, R. (2011): Paper electronics, Adv. Mater. 23, 1935–1961.

Torul, H., Çiftçi, H., Çetin, D., Suludere Z., Hakkı Boyacı, I., Tamer, U. (2015): Paper membrane-based SERS platform for the determination of glucose in blood samples, Anal. Bioanal. Chem. 407, 8243–8251.

Valtakari D., Stepien M., Haapanen, J., Teisala, H., Tuominen, M., Kuusipalo, J., Mäkelä, J.M., Toivakka, M., Saarinen, J.J. (2016): Planar fluidic channels on TiO_2 nanoparticle coated paperboard, Nord. Pulp Pap. Res. J. 31, 232-238.

Vella, S.J., Beattie, P., Cademartini, R., Laromaine, A., Martinez, A.W., Phillips, S.T., Mirica, K.A., Whitesides, G.M. (2012): Measuring markers of liver function using a micropatterned paper device designed for blood from a fingerstick, Anal. Chem. 84, 2883-2891.

Villa, J.E.L., Poppi, R.J. (2016): A portable SERS method for the determination of uric acid using a paper-based substrate and multivariate curve resolution, Analyst 141, 1966-1972.

Vyörykkä, J. (2004): Confocal Raman microscopy in chemical and physical characterization of coated and printed papers, PhD thesis, Helsinki University of Technology, Helsinki.

Vyörykkä, J., Juvonen, K., Bousfield, D., Vuorinen, T. (2004): Raman microscopy in lateral mapping of chemical and physical composition of paper coating, TAPPI J. 3, 19-24.

Yu, W.W., White, I.M. (2010): Inkjet printed surface enhanced Raman spectroscopy array on cellulose paper, Anal. Chem. 82, 9626-9630.

Yuen, C., Liu, Q. (2013): Optimization of Fe3O4@Ag nanoshells in magnetic field-enriched surface-enhanced resonance Raman scattering for malaria diagnosis, Analyst 138, 6494-6500.

Zhou, Y., Fuentes-Hernandez, C., Khan, T.M., Liu, J.C., Hsu, J., Shim, J.W., Dindar, A., Youngblood, J.P., Moon, R.J., Kippelen, B. (2014): Recyclable organic solar cells on cellulose nanocrystal substrates, Sci. Rep. 3, 1536.

Manuscript received November 7, 2016
Accepted May 8, 2017